CHAPTER VIII
FIXED-BED COLUMN OF ARSENIC REMOVAL FROM ADUEOUS SLOUTION USING NANO ZERO-VALENT IRON COATED ON DIATOMITE

The batch adsorption methods provide useful information on the application of adsorption to the removal. However the column adsorption methods give the most practical application of this process in wastewater treatment of the water filter system. The performance of packed beds column study is important to predict the column breakthrough of the adsorption, which controls the operation of the adsorbent and regeneration time. Therefore, in this research field is applied the best conditions of arsenic removal used to study the packed beds column.

8.1 Objectives

In this study, the adsorptions of As^{5+} and As^{3+} by nZVI-D_2 is investigated using packed beds column and confirm that it can be used practically in the industrial adsorption column.

8.2 Materials and methods

8.2.1 Materials

Diatomite powder with particle size of 150 micron was achieved from the North Thailand. Iron(III) sulphate ($FeSO_4 \cdot 7H_2O$), sodium borohydride ($NaBH_4$) and absolute ethanol were used in this study to obtain from Merck Company (Germany) and Ajax Finechem (Australia). All aqueous solutions were prepared with deionized water which is purified with Millipore Milli-Q Plus water purification system. For batch adsorption experiments, 1 mg/L of As^{5+} solution was prepared by dissolving $Na_2HAsO_4 \cdot 7H_2O$ and $NaAsO_2$ was used for solutions of As^{3+}. Finally, the initial pH was adjusted using hydrogen chloride and sodium hydroxide.

This paper is accepted to published in the journal Advanced Materials Research

8.2.2 Column studies

The packed beds column was studied using a glass column with internal diameter of 1.8 cm and length of 15 cm. A schematic of the experimental setup used for column study is shown in Fig.1. The experiments used to the weight of nZVI-D_2 about 1 g and initial As^{5+} and As^{3+} concentration of 1 mg/L and the solution was adjusted the initial pH as 6. The height of nZVI-D bed was 6 cm. Next, As^{5+} and As^{3+} solution was through the column by a peristaltic pump which has the flow rate 7.5 mL/min. All experiments were carried out under room temperature (30ºC). The suspensions were filtered with syringe Filter Nylon 0.45-µm membrane from the exit at time intervals (0-780 min). The concentration of As^{5+} and As^{3+} was determined by Graphite furnace atomic absorption spectrometry (GFAAS), Perkin Elmer series Analyst 880, United States.

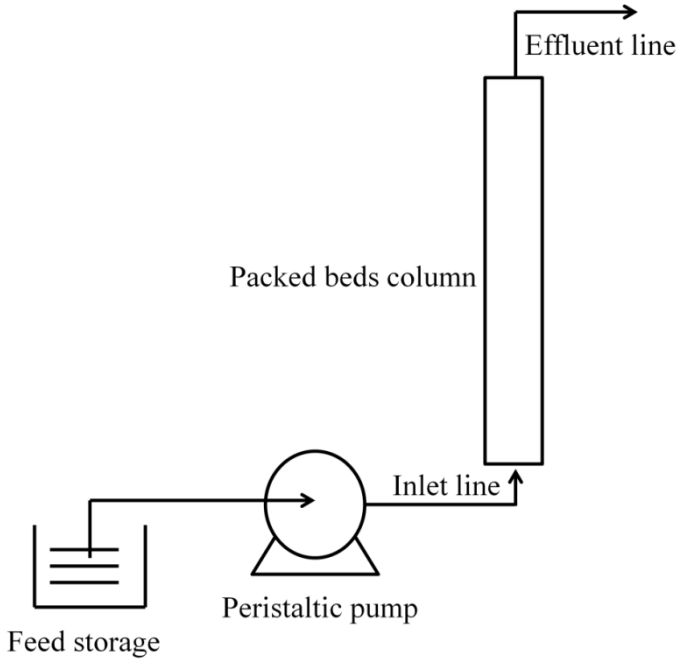

Figure 8.1 Schematic of the experimental setup for column study

The typical breakthrough curve is usually expressed by plotting $C_{effluent}$ or $C_{effluent}/C_{influent}$ versus treated service time t. Fig. 8.2 depicts a typical breakthrough curve where the column capacity is fully utilized. The concentration at breakthrough point is chosen arbitrarily at some low value, C_b. When the effluent concentration C_x

is approaching to 90% of C_0 (inlet adsorbate concentration) then the adsorbent is considered to be essentially exhausted (Goel, Kadirvelu, Rajagopal, & Kumar Garg, 2005). The capacity at exhaustion is determined by calculating the total area below the breakthrough curve. The column capacity (q_{column}) is estimated as follows (Öztürk & Kavak, 2005):

$$q_{column} = V \int_{tb}^{tx} \frac{(C_b - C_x)\, dt}{M} \tag{8.1}$$

where t_b, and t_x are the spent time system , C_b is influent metal concentration (mg/L), C_x is the effluent concentration at breakthrough point (mg/L) and V is volume flow rate.

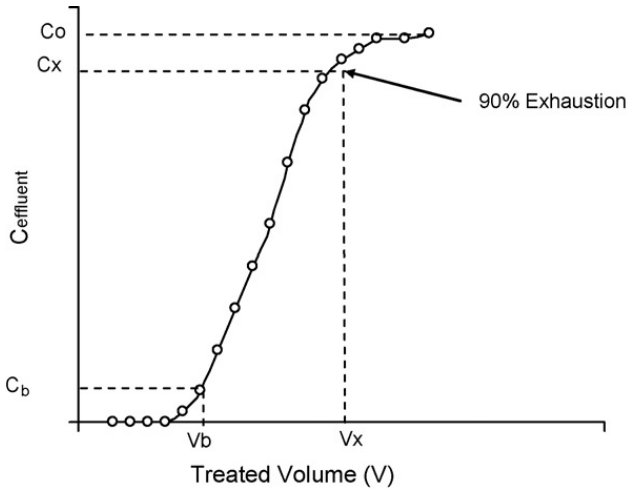

Figure 8.2 Ideal breakthrough curve (Bao et al., 1999)

The equilibrium metal uptake or adsorption capacity, q_e (mg/g) is calculated as shown in the following:

$$q_e = \frac{q_{column}}{M} \tag{8.1}$$

where M is the dry weight of nZVI-D_2 in the column (g).

8.3 Results and discussions

8.3.1 The performance of a packed beds column

The performance of a packed beds column can be described through the concept of breakthrough curve analysis. The time has influenced the breakthrough point and shape of the breakthrough curve. It is important characteristics for determining the operation and the dynamic responses of an adsorption column (Malkoc, Nuhoglu, & Dundar, 2006). In our previous batch adsorption show the suitable pH of As^{5+} and As^{3+} as pH 6, 1 mg/L of the initial concentration and 1 g of nZVI-D_2. The breakthrough curves are usually expressed in terms of adsorbed metal concentration. It defined the capacity at exhaustion is determined by calculating the total area below the breakthrough curve. The maximum column capacity (q_{column}; mg/g) of As^{5+} and As^{3+} were 2397.75 and 2010.89 µg/g, respectively (calculated by simpson equation). However, these capacities are still lower than the maximum equilibrium capacity at batch reactor of Langmuir models which the maximum adsorption capacity (q_{max}) was 2,801.65 and 2,682.04 µg/g of As^{5+} and As^{3+}, respectively. Due to, the flow rate in the column affected the mass transfer of cyanide as a result, the ability absorbed the decline.

The experimental breakthrough times at the flow rate 7.5 mL/min (corresponding to 0.01 of influent concentration), for As^{5+} and As^{3+} were found to be 90 and 100 min, respectively. The breakthrough time at 90 and 100 min, adsorption capacity is only 0.1% of all adsorption capacity in the case of As^{5+} and As^{3+}. Forasmuch, nZVI-D_2 is effective in the treatment of As^{5+} and As^{3+} which resulting the reaction time decreased, and also can result in As^{5+} and As^{3+} treatment has increased over a longer time. The exhaust times (corresponding to 95% of influent concentration) for As^{5+} and As^{3+} were found to be 510 and 570 min, respectively displayed Fig. 8.2(a-b). The results shown that As^{5+} has a residence time higher than As^{3+} all of the breakthrough times and the exhaust times (Maji, Pal, Pal, & Adak, 2007).

In fact, the breakthrough curves shown in Fig. 8(a-b) were not followed the typical “S-shape” curves that produced in ideal adsorption systems. The irregular breakthrough curves were obtained due to two factors: (a) the slow adsorption kinetics of cyanide on porous nZVI-D_2 (Khraisheh, Al-Degs, Allen, & Ahmad, 2002), where

the slow kinetics of cyanide makes the breakthrough faster and thus an incomplete "S" breakthrough shape is produced, and (b) the use of small-scale column tool usually produces unexpired breakthrough curves as reported in the literature (Al-Degs, Khraisheh, Allen, & Ahmad, 2009). However, this research breakthrough curves look similar S shape, indicating that the film diffusion and internal diffusion affect the system.

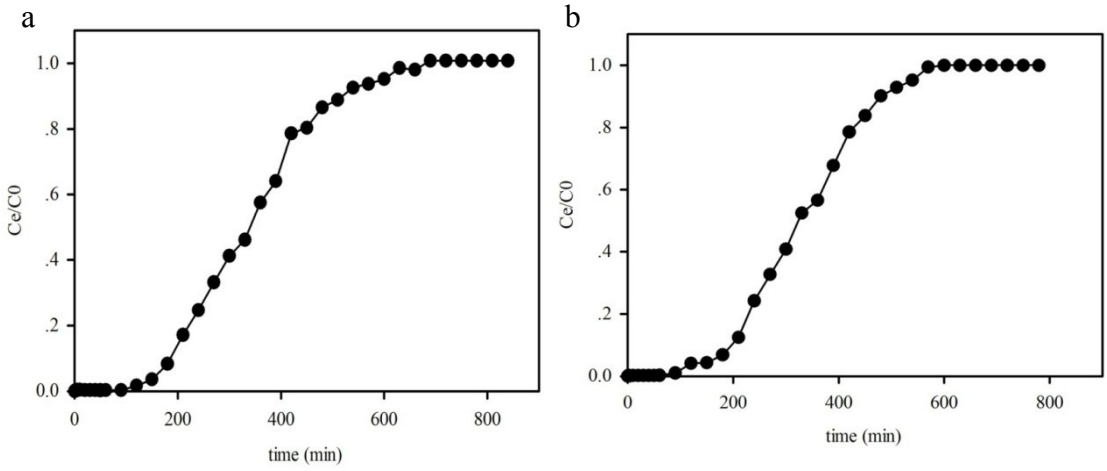

Figure 8.3 Breakthrough curves of (a) As^{5+} and (b) As^{3+} adsorption

8.3.2 Column dynamic studies

8.3.2.1 Application of the Thomas model

Thomas model has been applied by many researchers to study packed bed adsorption kinetics. It model disregard both the intra-particle mass transfer and the fluid film. This model is suitable for adsorption processes where the external and internal diffusion limitations between the adsorbate and the adsorbent (Saadi, Saadi, & Fazaeli, 2013; Sugashini & Sheriffa Begum, 2012). The maximum adsorption capacity was found in this model. The model has the following form

$$\ln\left(\frac{C_0}{C_e}-1\right)=\frac{K_{Th}q_e m}{Q}-K_{Th}C_0 t \tag{8.2}$$

where K_{Th} (mL/min mg) is the Thomas rate constant; q_e (mg/g) is the equilibrium As uptake per g of the adsorbent; C_o (mg/L) is the inlet As concentration; C_t (mg/L) is the

outlet concentration at time t; M (g) the mass of adsorbent, V (mL/min) the flow rate. The value of C_t/C_o is the ratio of outlet and inlet As concentrations. A linear plot of $ln[(C_o/C_t)-1]$ against time (t) was employed (figure not shown) to determine values of k_{Th} and q_e from the intercept and slope of the plot.

Table 8.1 Thomas model parameters at different conditions using linear regression analysis

	Initial concentrations (mg/L)	**bed height (cm)**	**Flow rate (mL/min)**	**k_{Th} (mL/min.mg)**	**q_e (µg/g)**	**R^2**
As^{3+}	1	0.6	7.5	1.344	2834.09	0.975
As^{5+}	1	0.6	7.5	2.050	2193.47	0.852

Table 8.1 lists the calculated Thomas constants from the experimental column data when the flow rate and initial influent concentration were varied. The correlation coefficient values of As^{5+} and As^{3+} were 0.852 and 0.975, respectively, indicate a good agreement between the experimental data and the column data generated using the Thomas model. The Thomas equation coefficients, K_{Th} are 2.050 and 1.344 L/min.mg. It is said that the adsorption As^{5+} and As^{3+} with packed beds column can predict the monolayer adsorption. Nonetheless, the As^{5+} was adsorption rate more than As^{3+}. Thomas model was suitable for the adsorption process further suggesting that both the external and internal diffusions will not be the limiting step (Chen et al., 2012). The decrease in K_{Th} values is due to the effect of driving force enhancement, whereas the increase of q_e is resulting from the higher number of adsorption sites with the increasing bed depth in the column.

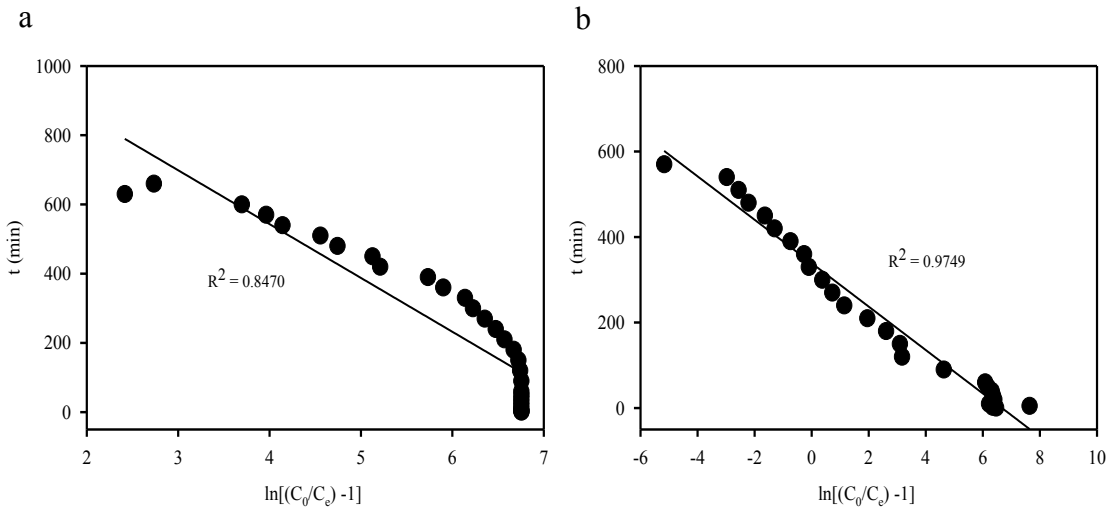

Figure 8.4 Thomas model kinetic plots for the adsorption of (a) As^{5+} and (b) As^{3+} on nZVI-D_2 (30ºC, pH 6, initial concentration: 1 mg/L and flow rate: 7.5 mL/min)

8.3.2.2 Application of the Yoon and Nelson model

This model is based on the assumption that the rate of decrease in the adsorption for each adsorbate molecule and the probability of adsorbate breakthrough on the adsorbent (Öztürk, & Kavak, 2005). The linearized form of the Yoon and Nelson model is as follows:

$$t = \tau + \frac{1}{K_{YN}} \ln \frac{C_e}{C_0 - C_e} \tag{8.3}$$

Where K_{YN} is the rate constant of Yoon and Nelson model (L/min), τ is the time required for 50% adsorbate breakthrough (min) and t is the breakthrough time (min).

The values of K_{YN}, τ and adsorption capacity was found plot of $lnC_e/(C_o-C_e)$ versus t shown Fig 8.6a-b. The Yoon and Nelson model model parameters for the adsorption of As^{5+} and As^{3+} onto the nZVI-D_2 were calculated using linear regression analysis and the results were presented in Table 3. The R^2 values 0.9727 and 0.9759 for As^{5+} and As^{3+} adsorption, respectively, indicating a good agreement and the justness of the Yoon and Nelson model. From Table 3, it is noted that the value of K_{YN} are 0.016 and 0.019 L/min and τ are 366.24 and 338.81

min for As^{5+} and As^{3+}, respectively. In short, the value K_{YN} of As^{3+} more than As^{5+} may be the driving force of As^{5+} less than As^{3+} in the liquid phase. This is consistent with breakthrough time which As^{5+} solution over time in column As^{3+}. Therefore, the process of As^{5+} and As^{3+} adsorption was obtained that the rate of decrease of adsorption for each adsorbate molecule is proportional of adsorbate adsorption and adsorbate breakthrough on the adsorbent.

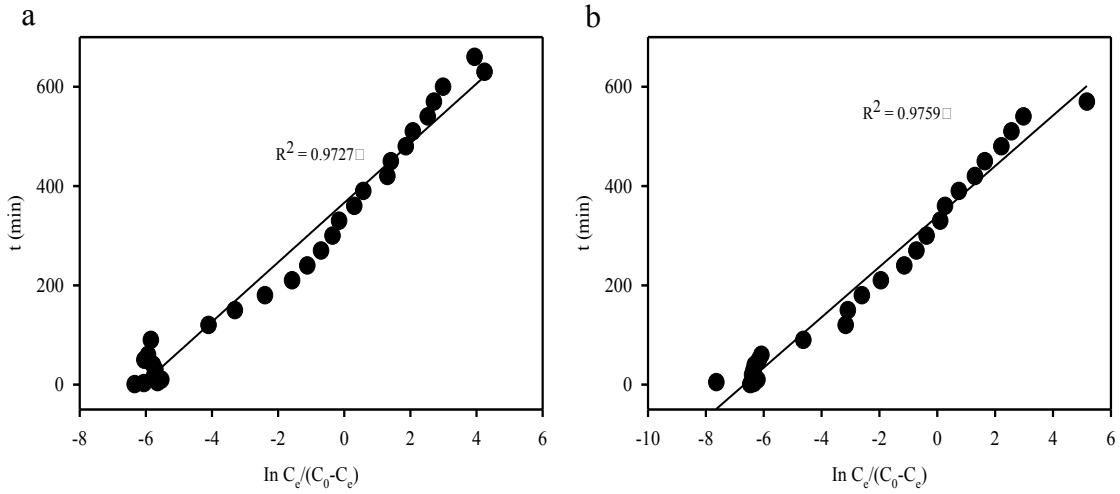

Figure 8.5 Yoon and Nelson model kinetic plot for the adsorption of (a) As^{5+} and (b) As^{3+} on nZVI-D_2 (30ºC, pH 6, initial concentration: 1 mg/L and flow rate: 7.5 mL/min)

Table 8.2 The Yoon and Nelson model parameters at different conditions using linear regression analysis

	Initial concentrations (mg/L)	**bed height (cm)**	**Flow rate (mL/min)**	**K_{YN} (mL/min.mg)**	**q_e (mg/g)**	**R^2**
As^{3+}	1	0.6	7.5	0.019	5619.58	0.975
As^{5+}	1	0.6	7.5	0.016	10939.3	0.972

In sum up, it can be concluded that both Thomas and Yoon-Nelson models are appropriate models to describe fixed-bed operations. The high values of correlation coefficients indicated that increase of the initial concentration increased

the competition between adsorbate molecules for the adsorption site (Xu et al., 2009). Therefore, the model and the constants estimated can be used for the design of adsorption columns for As^{5+} and As^{3+} adsorption by nZVI-D_2.

8.4 Conclusion

This study shows that the nZVI-D_2 could be suited as an effective low-lost adsorbent for the removal of As^{5+} and As^{3+} from aqueous solution in a fixed-bed column system. The maximum column capacity (q_{column}; mg/g) of As^{5+} and As^{3+} were 2397.75 and 2010.89 µg/g, respectively. The column experimental data were analyzed using Thomas and Yoon–Nelson models. The Thomas and Yoon–Nelson models were successfully applied in describing the dynamic behavior of the adsorption process. In summary, the nZVI-D_2 has significant potential as an adsorbent for the treatment As^{5+} and As^{3+} contaminated in wastewater.

8.5 List of abbreviations

τ	time required for 50% adsorbate breakthrough (min)
C_b	influent metal concentration (mg/L)
C_e	outlet metal concentration as a function of time or volume (mg/L)
C_0	inlet metal concentration as a function of time or volume (mg/L)
C_x	effluent concentration at breakthrough point (mg/L)
K_{Th}	Thomas rate constant (L/min. mg)
K_{YN}	rate constant of Yoon and Nelson model (L/min)
M	dry weight of nZVI-D in the column (g)
q_{column}	column capacity (mg/g)
q_e	equilibrium metal uptake or adsorption capacity (mg/g)
t_b	time spent system in influent (min)
t_x	time spent system in effluent (min)
V	volume flow rate

8.6 References

Al-Degs, Y.S., Khraisheh, M.A.M., Allen, S.J., & Ahmad, M.N. (2009). Adsorption characteristics of reactive dyes in columns of activated carbon. **Journal of Hazardous Materials, 165**(1–3), 944–949.

Bao, M. L., Griffini, O., Santianni, D., Barbieri, K., Burrini, D., & Pantani, F. (1999). Removal of bromate ion from water using granular activated carbon. **Water Research, 33**(13), 2959–2970.

Chen, S., Yue, Q., Gao, B., Li, Q., Xu, X., & Fu, K. (2012). Adsorption of hexavalent chromium from aqueous solution by modified corn stalk: a fixed-bed column study. **Bioresource Technology, 113,** 114–120.

Goel, J., Kadirvelu, K., Rajagopal, C., & Kumar Garg, V. (2005). Removal of lead(II) by adsorption using treated granular activated carbon: Batch and column studies. **Journal of Hazardous Materials, 125**(1–3), 211–220.

Khraisheh, M.A.M., Al-Degs, Y.S., Allen, S.J., & Ahmad, M.N. (2002). Elucidation of Controlling Steps of Reactive Dye Adsorption on Activated Carbon. **Industrial & Engineering Chemistry Research, 41**(6), 1651–1657.

Maji, S.K., Pal, A., Pal, T., & Adak, A. (2007). Modeling and fixed bed column adsorption of As(III) on laterite soil. **Separation and Purification Technology, 56**(3), 284–290.

Malkoc, E., Nuhoglu, Y., & Dundar, M. (2006). Adsorption of chromium(VI) on pomace—An olive oil industry waste: Batch and column studies. **Journal of Hazardous Materials, 138**(1), 142–151.

Öztürk, N., & Kavak, D. (2005). Adsorption of boron from aqueous solutions using fly ash: Batch and column studies. **Journal of Hazardous Materials, 127**(1–3), 81–88.

Saadi, Z., Saadi, R., & Fazaeli, R. (2013). Fixed-bed adsorption dynamics of Pb(II) adsorption from aqueous solution using nanostructured γ-alumina**. Journal of Nanostructure in Chemistry, 3**(1), 48.

Sugashini, S., & Sheriffa Begum, K.M.M. (2012). Column Adsorption Studies for the Removal of Cr(VI) Ions by Ethylamine Modified Chitosan Carbonized Rice Husk Composite Beads with Modelling and Optimization. **Journal of Chemistry.**

Xu, X., Gao, B., Wang, W., Yue, Q., Wang, Y., & Ni, S. (2009). Adsorption of phosphate from aqueous solutions onto modified wheat residue: Characteristics, kinetic and column studies. **Colloids and Surfaces B: Biointerfaces, 70**(1), 46–52.